A Diffusion-Reaction Model for α-Chymotrypsin Carrying Uniform Thermosensitive Gel Beads

A. TUNCEL

Hacettepe University, Chemical Engineering Department, 06532, Ankara, Turkey

Received 14 January 1998; accepted 19 March 1999

ABSTRACT: In this study, the kinetic behavior of α-chymotrypsin-immobilized, uniform poly(isopropylacrylamide) gel beads was investigated. The kinetic study was performed by using a continuous reactor operated at steady-state conditions. In the experiments, substrate feed concentration, residence time, and reactor temperature were changed. The results were explained by a diffusion–reaction model developed for steady-state conditions. The effectiveness factor and Thiele modulus values of the thermosensitive enzyme–gel system were estimated at different temperatures by using an iterative procedure based on fourth order Runge–Kutta algorithm. The results indicated that the overall hydrolysis rate was controlled by the substrate diffusion through the gel matrix. A bending point was detected for the Thiele modulus at the lower critical solution temperature (LCST) of the thermosensitive gel. The effective diffusion coefficient of substrate and effectiveness factor decreased suddenly at LCST. The mass transfer process within the thermosensitive carrier could be described in detail by the proposed model. The results of our numerical procedure were also compared with an analytical approximate solution available in the literature. The consistency between two different model was reasonably good. © 1999 John Wiley & Sons, Inc. J Appl Polym Sci 74: 1025–1034, 1999

Key words: isopropylacrylamide; chymotrypsin; physical entrapment; effectiveness factor; thermoresponsive gel; enzyme immobilization

INTRODUCTION

Thermosensitive gels have been proposed as alternative enzyme carriers by different investigators.[1–7] Crosslinked *N*-isopropylacrylamide–acrylamide copolymer gel microspheres were tried as a carrier in the immobilization of β-D-galactosidase.[2] The enzyme–gel system was examined in a continuous packed-bed reactor cycled between 30–35°C. It was shown that thermal cycling caused a significant increase in the immobilized enzyme activity relative to the isothermal operation. A crosslinked thermosensitive gel, poly(vinyl methyl ether) produced with γ-ray irradiation, was used in the immobilization of exo-1,4-α-D-glucosidase.[3] The on/off control of the hydrolysis of maltose could be achieved by this system. A biochemomechanical system was produced by the immobilization of urease within a thermosensitive *N*-isopropylacrylamide–acrylic acid copolymer gel.[4] In this system, the ammonia produced enzymatically interacted with the carboxyl groups of the gel, which in turn, induced the swelling process. Although the temperature was kept above the lower critical solution temperature of the gel, the urease–gel system was in the swollen state when it was exposed to urea. However, the gel could be collapsed reversibly in the absence of urea. Crosslinked poly(*N*-isopropylacrylamide) gel was also tried as a carrier in the im-

Correspondence to: A. Tuncel.

Journal of Applied Polymer Science, Vol. 74, 1025–1034 (1999)
 CCC 0021-8995/99/041025-10

mobilization of esterase.[5] Recently, lipase was covalently bound to a graft copolymer prepared by coupling of poly(acrylic acid-*co*-acrylamide) with poly(isopropylacrylamide), having an amino group at its end.[6] The catalytic activity of lipase immobilized to the graft copolymer had a bending point around 25–30°C in isopropanol–water medium.[6] Park and Hoffman proposed a preparation procedure for producing uniform, thermosensitive gel beads for use in biotechnological applications.[7]

In our previous studies, we produced different thermosensitive structures based on the copolymers of *N*-isopropylacrylamide.[8–11] The uniform microspheres made of crosslinked *N*-isopropylacrylamide were proposed as a carrier for the immobilization of α-chymotrypsin.[9] The batch reactor performance of α-chymotrypsin loaded uniform poly(*N*-isopropylacrylamide) microspheres was investigated elsewhere.[9] In this study, the same microspheres were used in a continuous stirred reactor operated at steady-state conditions. To describe the diffusion and reaction process within the gel microspheres, a steady-state diffusion–reaction model was applied on the continuous reactor data collected at different temperatures. The effective diffusion coefficient of synthetic substrate, the Thiele modulus, and effectiveness factors of the enzyme–gel system were estimated at different reaction temperatures.

EXPERIMENTAL

Materials

N-Isopropylacrylamide (NIPAM, Aldrich Chem. Co., Milwaukee, WI) was recrystallized from hexane–acetone solution. *N,N*-Methylenebisacrylamide (MBA, BDH Chemicals Ltd., UK) was the crosslinker. Potassium persulfate (KPS, BDH Chemicals Ltd.) and tetramethylethylenediamine (TEMED, Sigma Chem. Co., St. Louis, MO) were the initiator and the accelerator, respectively. Sodium alginate (medium viscosity, Sigma Chem. Co.) and calcium chloride (BDH Chemicals Ltd.) were used for the formation of alginate mold around the spherical gel beads. α-Chymotrypsin (CT, 52 μmol BTEE/mg protein-min) was supplied from Sigma Chemical Co. The activity of α-chymotrypsin was assayed by using a synthetic substrate, Benzoyl-L-Tyrosine Ethyl Ester (BTEE, Sigma Chemical Co.).

Preparation of Enzyme–Gel Beads

The detailed preparation procedure of the enzyme–gel beads was given elsewhere.[9] The beads encoded as CT-NIPAM1 and CT-NIPAM2 were prepared by dissolving 0.36 and 1.80 mg enzyme within the disperse phase including 3.6 mL water in both cases, respectively.[9] All of the produced amounts of CT-NIPAM1 and CT-NIPAM2 were used in the continuous stirred reactor runs. The respective enzyme loading values for CT-NIPAM1 and CT-NIPAM2 were determined as 73.12 and 78.89% of the initial enzymatic activity present in the gel formation medium.[9]

Characterization of Enzyme–Gel Beads

The surface morphology and the internal structure of the enzyme–gel beads were observed by a Scanning Electron Microscope (JEOL, JEM 1200EX, Japan).[9] For this purpose, the enzyme–gel beads were swollen to equilibrium in phosphate buffer solution at 15°C and subsequently freeze dried at −20°C. The freeze-dried beads were cut to obtain the cross-sectional view of the internal structure. The samples coated with a thin layer of gold (about 100 A) *in vacuo* were examined by a scanning electron microscope.

The equilibrium diameter of gel beads was measured at any particular temperature in an optical system constructed for this purpose.[9] The enzyme–gel beads coded as CT-NIPAM1 (prepared with 480 mg of NIPAM and 0.36 mg of CT, 3 mm in diameter in the production conditions) were used in these measurements performed in borate buffer at a pH of 7.8. The equilibrium swelling ratio (Θ) was expressed in the dimensionless form according to eq. (1):

$$\Theta = (d/d_o)^3 \tag{1}$$

where, d (mm) is the equilibrium diameter of gel beads at any temperature, and d_o (mm) is the diameter of gel beads at the production conditions. In these experiments, five beads were followed, and the mean of measured linear swelling ratios was calculated. The standard deviation of linear swelling ratio measurements with different particles was not higher than 5%.

Enzymatic Activity Experiments

The enzyme–gel particles were tried in a continuous stirred reactor equipped with a temperature control system. In most of the runs, the hydrolysis

medium at a pH of 7.8 included 95% borate buffer and 5% ethanol (by volume). To start the continuous run, the enzyme–gel beads in a Teflon basket were placed into the reactor containing 130 mL of hydrolysis medium with an initial BTEE concentration of 398.9 μM. Then the substrate solution including 398.9 μM BTEE was fed into the reactor. The inlet and outlet volumetric flow rates were set to 0.75 mL/min. The reactor was heated or cooled to the desired temperature while the hydrolysis medium was stirred magnetically at 300 rpm. The stirring of the hydrolysis medium was continued at least 2 h for reaching of the enzyme–gel beads to their equilibrium water content at the studied temperature. The absorbance of the outlet flow was continuously monitored at 258 nm by a UV-VIS spectrophotometer. After a certain time, the absorbance of outlet stream reached to a plateau value (i.e., steady-state absorbance). The runs were continued for at least 4 h after the steady-state conditions were attained within the reactor. After the run, the enzyme–gel beads were washed with 250 mL of fresh borate buffer (pH 7.8) by shaking the medium at 25°C for 1 h to remove any residual substrate or product within the gel matrix. The gel beads were stored in the refrigerator at +4°C within 250 mL of fresh borate buffer during the period between the continuous runs.

Determination of Immobilized Enzyme Activity

The observed hydrolysis rate with the enzyme–gel beads was calculated according to the eq. (2)

$$Q_{obs} = \upsilon C_0 X \tag{2}$$

where Q_{obs} is the observed hydrolysis rate (μmol BTEE/min), υ is the volumetric flow rate of the feed (L/min), C_0 is the BTEE feed concentration (μM BTEE), and X is the BTEE conversion achieved at steady state operation of the continuous reactor.

BTEE conversion was determined by using a spectrophotometric procedure that is very similar to that proposed by Clark and Bailey.[12] To determine the BTEE conversion, the absorbance values of the feed and product streams were measured in a UV spectrophotometer at the wavelength of 258 nm during the steady-state operation operation of the reactor. The following expression was used for the calculation of BTEE conversion

$$X = (A_{out} - A_{in})/\Delta A_{(x=1)} \tag{3}$$

where, A_{in} and A_{out} are the absorbance of the feed stream and the absorbance of the product stream in the steady-state operation of continuous reactor, respectively. $\Delta A_{(x=1)}$ is the absorbance difference corresponding to the complete conversion of substrate. For each substrate concentration, the difference values were determined in a batch reactor (130 mL) by using 0.36 mg free enzyme under identical conditions with the continuous reactor.

RESULTS AND DISCUSSION

The hydrolysis of a synthetic substrate (i.e., benzoyl-L-tyrosine ethyl ester, BTEE) was studied in a continuous stirred reactor including uniform and thermosensitive enzyme–gel beads. In the hydrolysis runs conducted at steady-state conditions, BTEE feed concentration, residence time, and reactor temperature were changed. The effects of these variables are presented below.

BTEE feed concentration was changed between 159.5–877.5 μM. These experiments were performed by using the enzyme–gel beads prepared with two different enzyme loading (i.e., CT-NIPAM1 and CT-NIPAM2). The inlet and outlet volumetric flow rates were set to 0.75 mL/min. The hydrolysis medium in the continuous reactor included 95% borate buffer and 5% ethanol. The temperature, pH, and the stirring rate was 25°C, 7.8, and 300 rpm, respectively. The variation of observed BTEE hydrolysis rate with the BTEE feed concentration is given in Figure 1 for enzyme–gel beads prepared with two different enzyme loading. Here, the enzyme loading was expressed by dividing the amount of enzyme immobilized by the total volume of the gel beads at the production conditions (i.e., 4.2 mL for both preparations). As seen here, the observed rate increased linearly with the increasing BTEE feed concentration in the examined range. However, at constant BTEE concentration, the observed hydrolysis rate with the enzyme–gel beads prepared using the enzyme loading of 338.1 μg/mL (i.e., CT-NIPAM2), was slightly higher relative to that prepared with the enzyme loading of 62.6 μg/mL. Although the enzyme loading was increased about 5.5-fold, the observed rate exhibited a slight increase. This result indicated the presence of strong internal mass transfer resistance

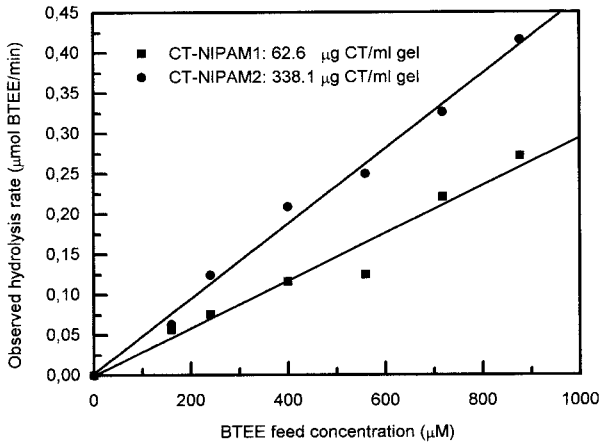

Figure 1 The variation of observed BTEE hydrolysis rate with the substrate feed concentration in the presence of enzyme–gel beads prepared by changing the enzyme loading.

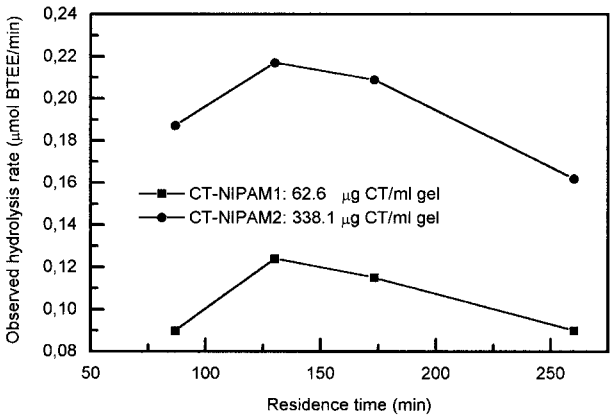

Figure 2 The variation of observed BTEE hydrolysis rate with the residence time in the presence of enzyme–gel beads prepared by changing the enzyme loading.

against the BTEE diffusion through the gel beads.

In the next set, the residence time was changed between 86.7–260 min in the continuous reactor having a constant volume 130 mL. Then, the residence time change could be achieved by changing the feed (also product) flow rate between 1.5 and 0.5 mL/min. The hydrolysis medium in the continuous reactor included 95% borate buffer and 5% ethanol. The temperature, pH, and the stirring rate was 25°C, 7.8, and 300 rpm, respectively. BTEE feed concentration was set to 398.9 μM in all runs performed the enzyme–gel beads prepared with two different enzyme loading (i.e., CT-NIPAM1 and CT-NIPAM2). The variation of observed BTEE hydrolysis rate with the residence time is given in Figure 2. Although a drastic change was not detected in the observed hydrolysis rate with the residence time, the variation exhibited a maximum point in the presence of both carriers. At the lowest and highest residence times, the observed hydrolysis rates were slightly lower. This tendency may be explained by the expression used for the calculation of observed hydrolysis rate. As stated above, eq. (2) was used for this calculation. For a constant BTEE concentration, magnitude of observed hydrolysis rate is controlled by the product of two variables (i.e., feed flow rate and BTEE conversion). In the continuous reactor runs the increase in the residence time was obtained by decreasing the feed flow rate at a constant reactor volume. A decrease in the volumetric flow rate involves a decrease in the observed hydrolysis rate, as seen in eq. (2). On the other hand, the variation of BTEE conversion with the residence time is given in Figure 3. As seen here, BTEE conversion increased by the increasing residence time (i.e., decreasing flow rate) for both cases. Therefore, the maximum value of the observed hydrolysis rate was obtained when the product of BTEE conversion and volumetric flow rate took a maximum value, according to eq. (2).

The reactor temperature was changed between 15–40°C by fixing the feed flow rate and BTEE feed concentration to 0.75 mL/min and 398.9 μM, respectively. The operating conditions and the initial composition of hydrolysis medium were the same with those of runs in which the effect of residence time was examined. The variation of observed hydrolysis rate with the temperature in

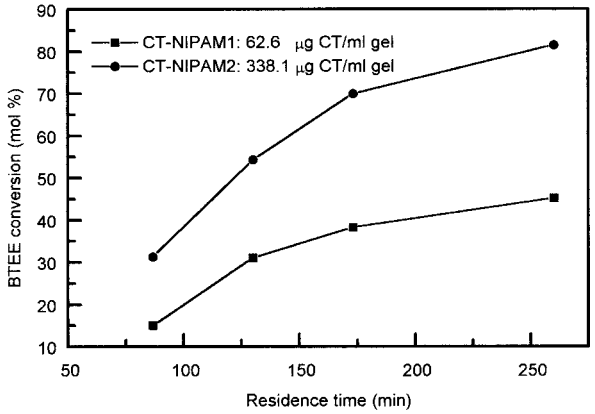

Figure 3 The variation of BTEE conversion with the residence time in the presence of enzyme–gel beads prepared by changing the enzyme loading.

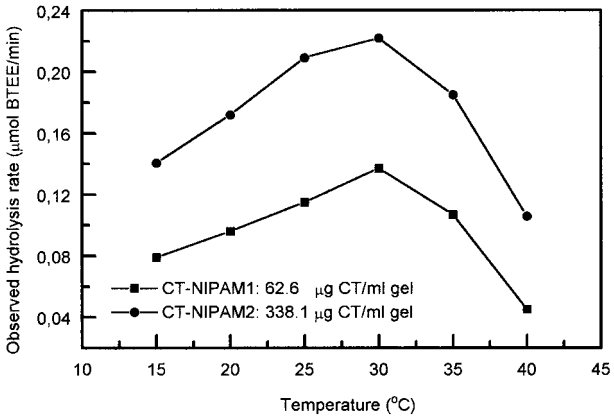

Figure 4 The variation of observed BTEE hydrolysis rate with the temperature in the presence of enzyme–gel beads prepared by changing the enzyme loading.

the presence of enzyme–gel beads prepared with two different enzyme loading is given in Figure 4. As seen here, the observed rate exhibited a maximum at 30°C in the continuous reactor for both types of carriers. The shapes of the curves in this figure were closely related to the thermosensitive properties of the carrier. The variation of the equilibrium swelling ratio of the gel beads with the temperature is given in Figure 5. As seen here, the gel volume continuously decreased with the increasing temperature and the lower critical solution temperature (LCST) of the enzyme–gel beads (i.e., a sharp decrease in the gel volume) was between 32–34°C.[9] It should be noted that the pores within the gel matrix become smaller, depending upon the decrease in the gel volume. Actually, the decrease in the pore size is not effective on the substrate diffusion rate up to a critical value of average pore size. In the swollen state of the gel matrix (i.e., at low temperatures), the size of pores are sufficiently large for the diffusion of substrate molecules. For this reason, although a decrease was observed in the gel volume, the observed hydrolysis rate increased in the temperature range of 15–30°C. This result possibly indicated that the magnitude of internal mass transfer resistance for substrate diffusion was possibly constant in the temperature range of 15–30°C. The increase in the observed hydrolysis rate up to 30°C may be explained by the dominant effect of increasing substrate conversion ability of immobilized enzyme with the increasing temperature. As seen in Figure 5, due to the drastic decrease in the gel volume occurred in the LCST of the gel matrix (i.e., between 32–34°C), the average pore size possibly decreased to a critical value that significantly prevented the diffusion of BTEE molecules into the gel. In other words, the internal mass transfer resistance against the substrate diffusion increased drastically at the temperatures higher than 30°C.[9] Then, the observed rate decreased sharply after 30°C. The kinetic behavior of the thermosensitive enzyme–gel system was quantified by a diffusion–reaction model to explain the observed tendency in Figure 4. The details of proposed model are given below.

Mathematical Model

At steady state, the mass balance equation for the diffusion of substrate through the gel matrix may be written as follows:[13]

$$\frac{D_e}{r^2}\frac{d}{dr}\frac{(r^2\,dC)}{dr} - \frac{r_m C}{K_m + C} = 0 \qquad (4)$$

In this equation, D_e is the effective diffusion coefficient of substrate within the gel microspheres, and C is the substrate concentration at any radial distance r. K_m and r_m are the Michealis–Menten kinetic parameters of the immobilized enzyme. Note that physical entrapment was used for the immobilization of α-chymotrypsin within the gel microspheres. Due to the nature of the selected immobilization method, it is expected that Michealis–Menten parameters of immobilized enzyme are roughly equal to the those of the free one. Therefore, an assumption was made by considering the equality of free and immobilized enzyme kinetic parameters. The enzyme loading

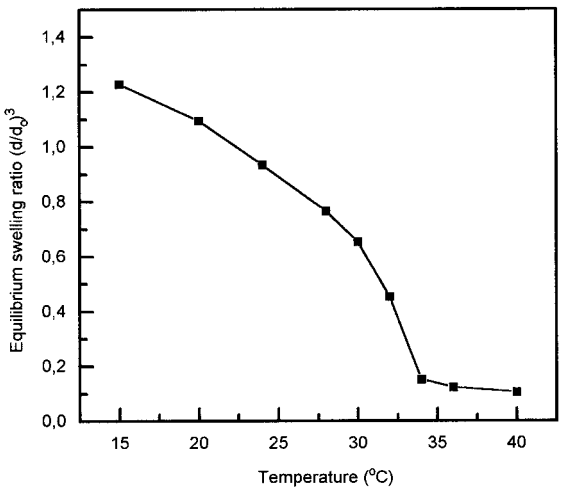

Figure 5 The variation of the equilibrium swelling ratio of the enzyme–gel beads with the temperature.

into the thermosensitive gel beads (m_{Ei}, mg/mL gel at any temperature) may be expressed by eq. (5),

$$m_{Ei} = M_{Ei}/V_{\text{gel}} \tag{5}$$

where M_{Ei} (mg) is the total amount of enzyme loaded into the gel microspheres, and V_{gel} is the gel volume, depending upon the temperature.

The maximum hydrolysis rate of the immobilized enzyme may be given by eq. (6).[13]

$$r_m = m_{Ei}V_m \tag{6}$$

where V_m is the maximum hydrolysis rate of free (or immobilized) enzyme expressed in terms of μmol BTEE converted by per mg enzyme per minute.

For the application of the mathematical model, the enzyme–gel microspheres prepared by using 0.36 mg of enzyme in the bead formation medium were selected. The enzyme leakage from the these microspheres were determined as 26.88% based on the initial activity present in the gel formation medium.[9] By taking into account the enzyme leakage, the total amount of enzyme loaded into the microspheres was calculated as 0.263 mg. In our previous study, the kinetic parameters of free enzyme [K_m (μM BTEE) and V_M (μmol BTEE/mg enzyme-min)] were determined at different temperatures by using 0.36 mg of free enzyme in a batch reactor having the same volume with the continuous one (i.e., 130 mL).[13] In these experiments, the initial substrate concentration was changed between 40–600 μM at the each temperature. pH and composition of the hydrolysis medium in the batch reactor were the same with the continuous one.[14] K_m and V_m values estimated from the Lineweaver–Burk plots sketched for each temperature were assumed to be equal to the those of the immobilized enzyme. The determined K_m and V_m values were also expressed as a function of temperature (T,°C) by using a polynomial-fitting algorithm based on the least-squares estimation. The relationships are presented below with their coefficient of variations (CV):

$$K_m = 205.1 + 0.0562T - 0.0264T^2 \qquad \text{CV} = 0.82 \tag{7}$$

$$V_m = 175.48 - 24.48T + 1.106T^2 - 0.013T^3 \qquad \text{CV} = 0.99 \tag{8}$$

Note that K_m of the free enzyme was reasonably insensitive to the temperature change in the range of 15–40°C. For this reason, a low CV value (i.e., 0.82) was obtained in the polynomial fitting for K_m because the total change in K_m was very small (i.e., about 5%). However, this relation could describe the experimentally determined K_m value within 1% accuracy at the studied temperatures. As seen in eq. (8), V_m could be expressed as a function of temperature with a sufficiently high CV value because it changes drastically by the temperature.

The diffusion and reaction model was not applied for the enzyme–gel microspheres prepared by using 1.80 mg of enzyme in the gel formation medium. To determine the free enzyme parameters with such a high amount of free enzyme in a batch reactor having a volume of 130 mL was reasonably difficult, because the time for complete conversion of BTEE was very short (i.e., less than 1–2 min in most cases). Therefore, the accurate determination of kinetic parameters could not be achieved in the presence of very high initial hydrolysis rates originated from the high amount of enzyme in the hydrolysis medium.

The boundary conditions of eq. (4) may be given as follows:

$$r = 0 \quad \frac{dC}{dr} = 0 \tag{9}$$

$$r = R \quad C = C_s \tag{10}$$

In eq. (10), R is the equilibrium radius of the thermosensitive gel microspheres at any temperature, and C_s is the substrate concentration on the surface of beads in the continuous reactor operated at steady-state conditions. By neglecting the external film-resistance around the beads in a well-mixed reactor, the surface substrate concentration may be assumed to be equal to the substrate concentration in the hydrolysis medium. This concentration value is also equal to the steady-state substrate concentration in the outlet stream. By using the following variables in eq. (11), eqs. (4), (9), and (10) may be expressed in the dimensionless form.

$$\zeta = r/R \quad \theta = C/C_s \tag{11}$$

Here, ζ and θ are the dimensionless radial distance and dimensionless substrate concentration within the gel beads, respectively.

$$\frac{1}{\zeta^2}\frac{d}{d\zeta}\frac{(\zeta^2 d\theta)}{d\zeta} - \frac{9\varphi^2\theta}{1+\beta\theta} = 0 \tag{12}$$

$$\zeta = 0 \quad \frac{d\theta}{d\zeta} = 0 \tag{13}$$

$$\zeta = 1 \quad \theta = 1 \tag{14}$$

In eq. (12), β is the ratio of surface substrate concentration to the K_m value of the enzyme.

$$\beta = C_s/K_m \tag{15}$$

where ϕ is the Thiele modulus of the thermosensitive gel beads and defined by eq. (16).

$$\varphi = (R/3)(r_m/K_m D_e)^{1/2} \tag{16}$$

The observed BTEE hydrolysis rate (Q_{obs}) with the thermosensitive enzyme–gel beads in a continuous reactor operated at steady-state may be predicted by eq. (17), where N is the number of the thermosensitive enzyme–gel beads present in the reactor. Here, it should be noted that the decrease in the surface area of the beads due to the decreasing radius with the increasing temperature was the another factor controlling the observed rate according to eq. (17).

$$Q_{\text{obs}} = +D_e 4\pi R^2 N \frac{(dC)_{r=R}}{dr} \tag{17}$$

Here, it should be noted that the observed BTEE hydrolysis rate may also be found from the experimentally measured variables as given in eq. (18).

$$Q_{\text{obs}} = \upsilon C_0 X_s \tag{18}$$

To solve eq. (12), including an unknown Thiele modulus value, with the boundary conditions of (13) and (14), an iterative algorithm written in Basic language was run in an IBM computer. The iterative procedure was started with an assumed value of the Thiele modulus. Then, the solution of eq. (12) was performed by using Fourth Order Runge–Kutta algorithm with the step size of 0.0005. In the algorithm, the Thiele modulus was changed until the correct value was found. To terminate the iterations, the equality of observed hydrolysis rate predicted by eq. (17) to the experimentally determined value was checked. The following expression was utilized for this purpose. Equation (17) (i.e., predicted form of the observed hydrolysis rate) was equated to eq. (18) (i.e., experimentally determined form of the observed hydrolysis rate). Equation (19) was obtained by introducing dimensionless radial distance and dimensionless BTEE concentration into the resulting expression.

$$\frac{(d\theta)_{\zeta=1}}{d\zeta} = \frac{\upsilon X}{4\pi R N D_e}(C_0/C_s) \tag{19}$$

The substitution of effective diffusion coefficient from the definition of the Thiele modulus into eq. (19) yielded eq. (20).

$$\frac{(d\theta)_{\zeta=1}}{d\zeta} = \frac{9K_m\varphi^2\upsilon X}{4\pi R^3 N V_m}(C_0/C_s) \tag{20}$$

When, the dimensionless concentration derivative at the surface of the gel beads was equal to the right side of eq. (20), the iteration was terminated and the Thiele modulus providing this equality with 1% accuracy was taken as the correct value. As given in eq. (21), this criterion was used in the program by taking the ratio of left side of eq. (20) to its right side. When this ratio was between 0.99 and 1.01, the iteration was terminated. After estimation of the Thiele modulus for a certain reactor temperature, the effective diffusion coefficient of BTEE was calculated by eq. (16).

$$\left[\frac{(d\theta)_{\zeta=1}}{d\zeta}\right] \Big/ \left[\frac{9K_m\varphi^2\upsilon X}{4\pi R^3 N V_m}(C_0/C_s)\right] = 0.99\text{–}1.01 \tag{21}$$

By the evaluation of dimensionless BTEE concentration profiles within the gel beads, the observed BTEE hydrolysis rates based on the variable gel volume (μmol BTEE/min-mL gel at any temperature) were calculated for different temperatures by using eq. (22).[15]

$$R_{\text{obs}} = 3V_m\beta\int_0^1 \frac{\zeta^2\theta}{1+\beta\theta}\,d\zeta \tag{22}$$

Effectiveness factor of the thermosensitive enzyme–gel beads may be given by eq. (23).

$$\eta = Q_{\text{obs}}/Q_s \tag{23}$$

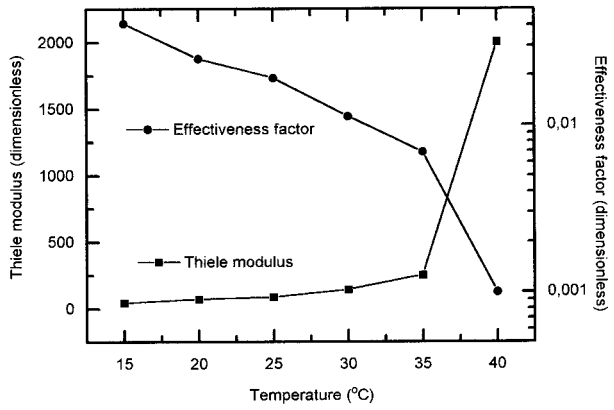

Figure 6 The variation of Thiele modulus and effectiveness factor values of the enzyme–gel system with the temperature of the hydrolysis medium.

In eq. (23), Q_{obs} and Q_s (μmol BTEE/min) were the observed hydrolysis rate and the hydrolysis rate at the surface concentration of substrate, respectively. Equation (23) may also be expressed in the following form.

$$\eta = \frac{D_e 4\pi R^2 N (dC/dr)_{r=R}}{(4/3)\pi R^3 N \dfrac{r_m C_s}{K_m + C_s}} \tag{24}$$

For the numerical procedure, the effectiveness factor was expressed in terms of dimensionless variables as given in eq. (25).

$$\eta = \frac{(1+\beta)}{3\varphi^2} (d\theta/d\zeta)_{\zeta=1} \tag{25}$$

The Thiele modulus and effectiveness factors estimated by the iterative algorithm were plotted against the hydrolysis temperature in Figure 6. As seen here, there was a bending point in the Thiele modulus of the enzyme–gel system at 35°C. The Thiele modulus value at 40°C was significantly higher relative to that observed at 35°C. Then, a sudden increase in the Thiele modulus was observed after the LCST of the gel matrix. Although a fourfold decrease was observed for the effectiveness factor in the temperature range of 15–35°C, the decrease between 35–40°C was about sevenfold. This result indicated that a sudden decrease was also observed for the effectiveness factor after the LCST value of the gel matrix. A reasonably higher Thiele modulus and lower effectiveness factor values clearly indicated that the overall hydrolysis rate with the enzyme–gel beads was controlled by the internal mass transfer resistance against the substrate diffusion. The variation of effective diffusion coefficient of substrate by the hydrolysis temperature is given in Figure 7. As seen here, a drastic decrease occurred in the effective diffusion coefficient after 35°C, while it was decreasing slightly in the temperature range of 15–35°C. By considering the definitions of the Thiele modulus and effectiveness factor [i.e., eqs. (16) and (25)], the sudden increase in the Thiele modulus and the sudden decrease in the effectiveness factor at the temperatures higher than LCST may be explained by the sudden decrease occurred in the effective diffusion coefficient of substrate after 35°C. The decrease in the effective diffusion coefficient is directly related to the shrinking of the gel matrix by the increasing the temperature. A representative SEM photograph indicating the surface and the interior of uniform gel beads is given in Figure 8. As mentioned elsewhere, the gel beads were composed of two different parts, namely, a highly porous interior, and a shell layer, with reasonably lower porosity as the exterior bead surface.[9] The dimensionless BTEE concentration profiles determined by the numerical solution of eq. (12) may be useful for understanding which part of the gel beads was effective for controlling the substrate diffusion rate within the gel matrix. The dimensionless BTEE concentration profiles within the gel matrix are given in Figure 9 for each hydrolysis temperature. As seen here, only 1% of the bead radius was used as the x-axis of the graph. In all temperatures, BTEE concentration decreased immediately after the

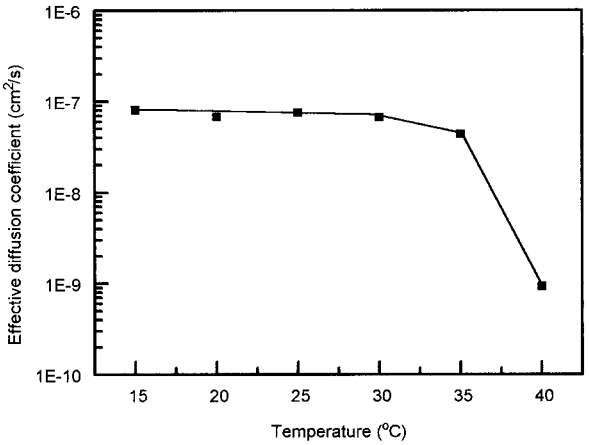

Figure 7 The variation of estimated effective diffusion coefficient of substrate with the reactor temperature.

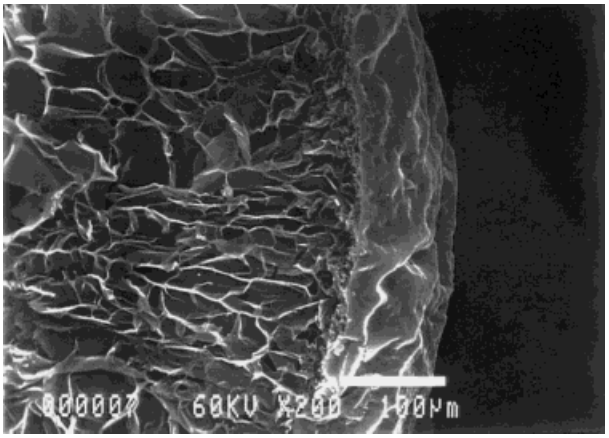

Figure 8 The SEM photograph showing the internal structure and the surface of enzyme loaded uniform NIPAM gel beads. Magnification:158×.

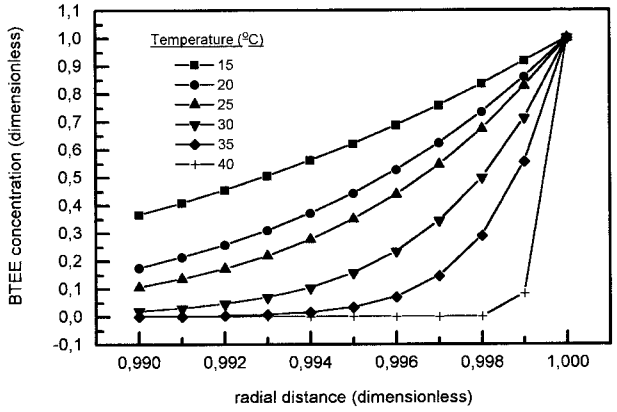

Figure 9 The dimensionless substrate concentration profiles within the thermosensitive gel matrix at different hydrolysis temperatures.

exterior surface and reached reasonably low values within 1% of the bead radius at any temperature. As seen in the SEM photograph, the thickness of shell layer around the macroporous interior was about 5 μm. One percent of the bead radius roughly corresponded to 15 μm for a gel bead having a 3-mm diameter in the production conditions. One percent of the bead radius mainly included the shell layer and a small part of the macroporous interior. By considering the BTEE concentration profiles shown in Figure 8, it could be stated that the hydrolysis reaction was completed mainly within the shell layer, and the substrate could not penetrate into the macroporous interior of the gel beads. Reasonably high enzyme content of the enzyme gel beads (i.e., 0.263 mg) was possibly responsible for this behavior. The shell layer was possibly in the form of an interpenetrating network including crosslinked isopropylacrylamide and alginate chains due to the production method of thermosensitive enzyme–gel beads.[9] Although it contained alginate chains, the shell layer exhibited a thermosensitive character because the diameter of enzyme–gel beads decreased with the increasing temperature.[9] Therefore, the closing of pores on the shell layer resulted in a decrease in the effective diffusion coefficient of substrate by increasing the temperature. To verify the model results, the hydrolysis rates (based on the gel volume) predicted with eq. (22) were compared with the experimentally determined ones. The experimental values were computed by using eq. (26).

$$R_{(\mathrm{exp})} = \upsilon C_0 / X / V_{\mathrm{gel}} \tag{26}$$

The results are given in Table I. As seen here, the consistency between the predicted and experimentally determined BTEE hydrolysis rates (based on the gel volume) was reasonably good. This consistency indicated that the estimation of the Thiele modulus and the solution of eq. (12)

Table I The Comparision of Calculated and Observed BTEE Hydrolysis Rates

Temperature (°C)	$R_{\mathrm{calc}} \times 10^2$ (μmol BTEE/mL gel-min)	$R_{\mathrm{exp}} \times 10^2$ (μmol BTEE/mL gel-min)
15	1.528	1.537
20	2.098	2.087
25	3.170	3.138
30	4.995	4.954
35	18.495	18.316
40	5.086	4.938

Table II Thiele Modulus Values Estimated by Approximate Analytical Solution and the Numerical Procedure Used in this Study

T (°C)	φ_{ns}	φ_{aas}	η_{exp}	η_{ns}
15	42.4	42.4	0.0412	0.0410
20	69.3	69.9	0.0250	0.0252
25	86.0	86.6	0.0191	0.0192
30	141.4	142.7	0.0112	0.0113
35	251.0	251.4	0.0069	0.0069
40	2002.0	2016.7	0.0009	0.0010

T, temperature; φ_{ns}, Thiele modulus from numerical procedure; φ_{aas}, Thiele modulus from approximate analytical solution; η_{exp}, experimentally determined effectiveness factor; η_{ns}, effectiveness factor determined by the numerical procedure.

could be performed correctly at the each temperature.

On the other hand, an approximate analytical solution for diffusion limited case was also available in the literature.[13] In the approximate solution, it was assumed that all substrate was utilized in a thin region within the bead adjacent to its exterior surface.[13] The validity of this assumption was shown with the substrate concentration profiles determined by the iterative procedure (i.e., Fig. 9). Then, the effect of curvature in spherical geometry was neglected in the transport equation of substrate. Based on this approximation, the evaluation of transport equation of substrate yielded the following expression between effectiveness factor and the Thiele modulus of a spherical enzyme carrier.[13]

$$\eta_{\varphi \gg 1} = (1/\varphi)\{(1 + \beta)/\beta\}2^{1/2}\{\beta - \ln(1 + \beta)\}^{1/2} \quad (27)$$

As seen in eq. (27), this expression is valid for the large values of the Thiele modulus. To estimate these values by the approximate solution, the effectiveness factors at different temperatures were calculated by using experimental data according to the following expression.

$$\eta = \{\upsilon C_0 X/V_{gel}\}/\{r_m \beta/(1 + \beta)\} \quad (28)$$

Experimentally determined the effectiveness factors and the Thiele modulus values from the approximate solution [i.e., from eq. (27)] are given in Table II. Both the effectiveness factors and the Thiele modulus values estimated by our model are also included in Table II. As seen here, the Thiele modulus values from the iterative procedure were very close to those found by the approximate solution. This result indicated that approximate analytical solution was also valid for the enzyme–gel system used in this study.

REFERENCES

1. Dong, L. C.; Hoffman, A. S. J Controlled Release 1986, 4, 223.
2. Park, T. G.; Hoffman, A. S. J Biomed Mater Res 1990, 24, 21.
3. Kokufuta, K. In Advances in Polymer Science: Responsive Gels, Volume Transitions II; Dusek, K., Ed.; Springer Verlag: Berlin, 1993, p. 167.
4. Kokufuta, E.; Zhang, Y. Q.; Ilmain, F.; Tanaka, T. Polym Prep Jpn 1991,. 40, 4204.
5. Kokufuta, E.; Tanaka, T. Macromolecules 1991, 24, 1605.
6. Takeuchi, S.; Omodaka, I.; Hasegawa, K.; Maeda, Y.; Kitano, H. Macromol Chem 1993, 194, 1991.
7. Park, T. G.; Hoffman, A. S. J Polym Sci Part A Polym Chem Ed 1992, 30, 505.
8. Senel, S.; Isik-Yuruksoy, B.; Cicek, H.; Tuncel, A. J Appl Polym Sci 1997, 64, 1775.
9. Bayhan, M.; Tuncel, A. J Appl Polym Sci 1998, 67, 1127.
10. Cicek, H.; Tuncel, A. J Polym Sci Part A Polym Chem 1998, 36, 527.
11. Cicek, H.; Tuncel, A. J Polym Sci Part A Polym Chem 1998, 36, 543.
12. Clark, D. S.; Bailey, J. E. Biotechnol Bioeng 1983, 25, 1027.
13. Bailey, J. E.; Ollis, D. F. Biochemical Engineering Fundamentals; McGraw-Hill: New York, 1986, p. 210, 2nd ed.
14. Tuncel, A. J Biotechnol 1998, 63, 41.
15. Scraton, R. E. NBasic Numerical Methods; Edward-Arnold: London, 1984, p. 53, 1st ed.